Technical Paper

ISSN 1997-1400 Int. J. Pavement Res. Technol. 5(4):245-256

Establishing Built-in Temperature Gradient for Jointed Plain Concrete Pavements in Pennsylvania

Somayeh Nassiri[1] and Julie M. Vandenbossche[1+]

Abstract: Temperature and moisture gradients that develop in concrete slabs are in twofold, transient and permanent. The slab curls in response to transient temperature gradients and warps in the presence of reversible drying shrinkage gradients. Permanent or built-in gradients include gradients that lock into the slab during hardening. Permanent gradients influence the transient curling/warping of the slab and need to be quantified. A method is proposed in this paper to establish the built-in temperature gradients for jointed plain concrete pavements (JPCPs) constructed in Pennsylvania. This method is based on the data from four instrumented JPCP projects in Pennsylvania. A temperature model is used as part of this study to estimate the built-in temperature gradient based on the climatic conditions of the paving site and the heat of hydration. The state is divided into three main climatic regions based on climatic indices and elevation of the counties across the state. Using the temperature model, the built-in temperature gradient is determined for JPCPs constructed in the three climatic regions, in different months during the construction season and at two different times of the day.

***Key words**: Built-in temperature gradient; Curling; Jointed plain concrete pavement; Slab.*

Introduction

The Portland cement concrete (PCC) slab in a pavement structure is exposed to different conditions at the surface in comparison to the bottom. At the top, the slab is directly exposed to the atmosphere, hence has to remain in balance with the ambient temperature and relative humidity. This results in daily temperature fluctuations and also evaporation and drying in the upper portion of the slab. At the bottom, the slab is in contact with the subgrade or base layer, and experiences less change in both temperature and moisture content. As a result of these different boundary conditions, temperature and moisture gradients are present throughout the slab thickness. In response to these gradients, the slab tends to curl toward the cooler and drier surface [1, 2]. This means that, when the surface of the slab is cooler than the bottom, known as a negative temperature gradient, the slab curls upward. Also, generally, the upper two inches (50 mm) of the slab is drier with respect to the remaining slab thickness [3]. This nonlinearity in the distribution of moisture throughout the slab also causes an upward curvature in the slab, known as warping. Studies have shown that while temperature gradients reverse on a daily basis, moisture gradients generally show seasonal fluctuations [4].

It has been shown that the slab does not necessarily remain flat in the absence of temperature and moisture gradients [5]. This reveals the effects of a third gradient in the slab, cited in literature with different names such as the built-in, construction, zero-stress, zero-deformation and permanent curling gradient. This is the temperature and/or moisture gradient present in the slab at the zero-stress time. The newly placed slab, although experiencing gradients throughout its depth, is not sufficiently stiff to overcome the constraints provided by its weight or the base layer, hence remains flat at the zero-stress time (TZ). The TZ takes place relatively shortly after the placement of the slab, proceeding final set time. The gradient present at TZ lock into the slab and, depending on the magnitude, increases or decreases the future curling of the slab due to transient gradients. It must be remarked that the built-in temperature gradient also includes the effects of permanent warping caused by irreversible drying shrinkage in the upper portion of the slab. This study, however, only focuses on the temperature portion of the built-in gradient and the methodology for estimating permanent warping can be found in another study [6].

The magnitude of the built-in temperature gradient depends strongly on the time and month of paving. Warm days with zero chance of the concrete freezing are typically selected for constructing pavements. Paving usually starts in the morning and continues throughout the day, depending on the paving production rate and length of the route. The portion of the road paved in the morning, typically reaches TZ in the evening (depending on the ambient conditions and the PCC mixture design) and slabs placed in the late afternoon most likely reach TZ during the following morning. The morning slabs end up with a negative built-in temperature gradient; hence experience less daytime downward curling and more enhanced upward curvature during the night.

Significance of Estimating Built-in Gradients

Both transient and built-in gradients play significant roles with regards to the performance of the pavement over the design life. This is because curling and warping of the slab are associated directly with the development of tensile stresses in the slab. In the case of upward curvature, the slab loses supports near the edges and the self-weight of the slab exerts tensile stresses near the top of the slab. Conversely, when curled downward, support is lost near the center of the slab and the self-weight of the slab exerts tensile stresses near the bottom of the slab. These stresses in combination with stresses generated from traffic loads can result in damage,

[1] University of Pittsburgh, 3700 Benedum Hall, Department of Civil and Environmental Engineering, 15261, Pittsburgh, PA, USA.

[+] Corresponding Author: E-mail jmv7@pitt.edu

Note: Submitted November 15, 2011; Revised February 11, 2012; Accepted February 22, 2012.

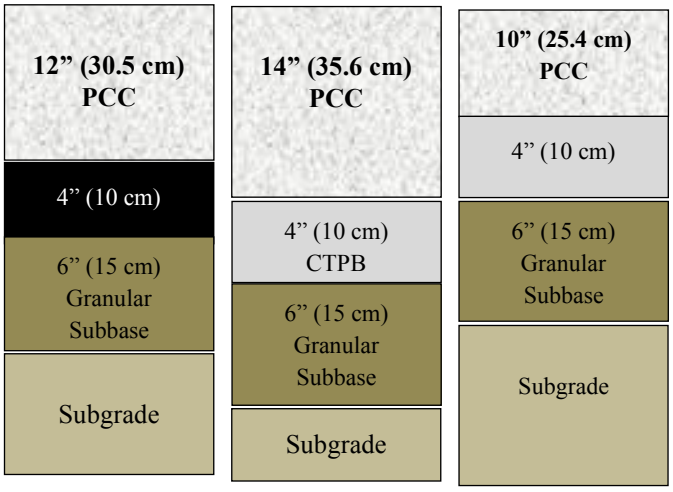

Fig. 1. Schematic View of the Pavement Structure for (a) Project 1 Paved on 9/2/2009 and Project 4 Paved on 5/10/2010, (b) Project 2 Paved on 10/8/2009, (c) Project 3 Paved on 4/29/2010 and 4/30/2010. (ATPB: Asphalt Treated Permeable Base; and CTPB: Cement Treated Permeable Base).

which accumulates over time until cracking develops.

The significance of curling and warping in the slab is better realized, when considering the recent evolution in the concrete pavement design from empirical procedures to mechanistic-based models. The mechanistic design of the slab requires a thorough knowledge of the shape of the slab, state and level of stresses in the slab at every loading cycle. This implies that both transient and permanent curling and warping need to be determined in the slab.

Currently, no theoretical procedure is available to estimate the built-temperature gradient in the slab. Previous attempts toward the determination of this parameter include the optimization of the cracking model incorporated into the Mechanistic-Empirical Pavement Design Guide (MEPDG) [7]. Also, a statistical study conducted by the Applied Research Associates (ARA) Consultant is a recent effort toward the characterization of the built-in temperature gradient [8]. This study suggests correlations for estimating the built-in gradient based on influential factors. The method again includes selecting a value for the built-in gradient based on the best agreement seen between the cracking predicted using the MEPDG and cracking observed in the LTPP sections. A direct and simple theoretical method that considers the effects of climatic conditions during paving, day and time of paving and also the PCC mixture design is yet to be developed.

The present study presents a practical procedure that considers the specifics of any individual JPCP project and predicts appropriate values for the built-in temperature gradient. The procedure is built upon the strain and temperature data from four instrumented paving projects in Western Pennsylvania. The four projects were constructed in the spring and summer of 2009 and 2010. The proposed procedure is then extended to be applicable to any JPCP constructed throughout the state. To overcome the need to instrument each pavement, a temperature model is developed and validated as part of the study. The validated temperature model is used to generate a chart containing the built-in temperature gradient for JPCPs constructed in different climatic regions in Pennsylvania, for each month during the construction season. The built-in temperature was established based on morning and afternoon paving for each month.

Test Sections Location and Instrumentation

Four different concrete paving projects, constructed in Pennsylvania during the summer/fall of 2009 and spring of 2010 were instrumented prior to paving. The projects were all part of the State Route (SR) 22 renewal project conducted by the Pennsylvania Department of Transportation (PennDOT). All projects are JPCPs with 12 by 15 ft (3.6 by 5.7 m) PCC slabs, 1.5 inch (38 mm) dowel bars along the transverse joints and No. 5 tie bars along the longitudinal joints along the shoulder and centerline. The structure of the four projects, including the average as-built thickness of the PCC slab, is presented schematically in Fig. 1. The projects are named based on the sequence of paving. The details regarding the mixture design and fresh and hardened concrete properties is summarized in Table 1 for the paving concrete used for each project. Two adjacent lanes were placed by a paver and curing compound was applied to the surface of all four projects immediately after construction. More details on the construction procedure and materials for the projects can be found in another reference [6].

Each instrumented project included nine slabs, divided into three groups (cells) of slabs. Each cell consists of three consecutive slabs. The three cells were located approximately at the start, middle and end of the paving day. Following this strategy provided the three different paving times of AM, noon and late PM for each project. A schematic layout of the instrumented projects is provided in Fig. 2.

Thermocouples and vibrating wire (VW) static strain gages were installed at different depths of the slabs. Type T thermocouples from Omega Engineering were installed at slab center and at different depths of the first and third slabs, referred to as Slabs A and C, in each cell. The as-built location of the thermocouples installed in the PCC layer for all projects is summarized in Table 2. Also, one extra thermocouple was installed at the mid-depth of the base and one approximately one foot (30 cm) into the subgrade in all projects. Two Geokon 4200 VW static strain gages were installed in the longitudinal direction at the center of all nine slabs in each project. The two gages in each slab were installed approximately one inch (2.54 cm) from the slab surface and one inch (2.54 cm) from the surface of the base. The gages were used to measure the axial strain and also temperature changes at the top and bottom of each slab. Major meteorological indices such as ambient temperature, relative humidity, solar radiation and wind speed and direction were also measured at the site for each project using a portable weather station.

Establishing Built-in Temperature Gradients for Instrumentation Projects

Establishing TZ

Since the built-in temperature gradient is the temperature and moisture gradient present in the slab at the TZ, this point in time needs to be identified for the slab. A methodology developed in a

Table 1. PCC Mixture Design, Fresh and Hardened Concrete Properties for all Projects.

	Project 1			Project 2			Project 3			Project 4		
	Cell 1	Cell 2	Cell 3	Cell 1	Cell 2	Cell 3	Cell 1	Cell 2	Cell 3	Cell 1	Cell 2	Cell 3
PCC Mixture Design (kg/m^3)												
Cement-Type I	297	297	297	326	326	326	297	297	297	297	297	297
Fly Ash	52	52	52	59	59	59	52	52	52	52	52	52
Fine Aggregate	791	784	772	688	688	690	691	691	691	780	762	772
Coarse Aggregate	1101	1099	1101	1091	1091	1091	1091	1091	1091	1103	1103	1099
Water Content	95	104	102	85	85	85	107	115	111	89	97	102
Cement Composition (%)												
SiO_2		20.2			19.5			20.7			20.1	
Al_2O_3		5.3			4.8			4.5			5.35	
Fe_2O_3		4.3			3.6			3.2			4.4	
CaO		64.4			52			63.1			63.4	
MgO		1.0			2.7			2.8			1.0	
SO_3		2.95			2.9			2.7			2.85	
C_3S		59			69			59			54.9	
C_2S					12			12				
C_3A		6.7			1			6				
Alkalis		0.55						0.66			0.53	
Blaine (m^2/kg)		380			403			390.9			358	
Fresh Mix Properties												
Slump (mm)	42	38	38	38	32	22	38	44	32	44	32	32
Entrained Air (%)	6.2	5.25	6.5	5.5	5.9	5.8	6.8	7.2	5.8	6	5.75	6
Unit weight (kg/m^3)	2435	2435	NA	2387	2411	2395	2371	2403	2371	2355	2403	2371
w/cm Ratio	0.41	0.475	0.47	0.48	0.5	0.46	0.47	0.46	0.46	0.46	-	0.48
Initial Set Time (Hours)		4.5			5.6			6.8			5.6	
Final Set Time (Hours)		5.7			7.6			9.4			7.3	
28-day Strength Properties												
Elastic Modulus, MPa	36883	34125	32402	27921	29300	33091	28955	30678	29644	35849	33781	34125
Poisson's Ratio	0.2	0.2	0.2	0.2	0.2	0.2	0.2	0.2	0.2	0.2	0.2	0.2
Compressive Strength, MPa	39.9	39.5	33.2	33.8	33.4	36.3	31.6	34.5	35.1	40.6	39.5	44.4
Flexural Strength, MPa	6.4	6.5	5.4	5.3	4.9	6.0	5.9	5.1	5.4	5.9	5.0	5.8

previous study based on the strain-temperature behavior of the slab was used to establish the TZ [9]. In this methodology, TZ is defined as the transition point in the strain-temperature response of the slab, as the concrete gradually transforms from a thixotropic material capable of flow to a hardened, rigid material. TZ was established for all four projects following this methodology. This task is discussed further in another study by the authors [6] and is therefore not elaborated upon here. A summary of the TZs established for each cell in each of the projects is summarized in Table 3.

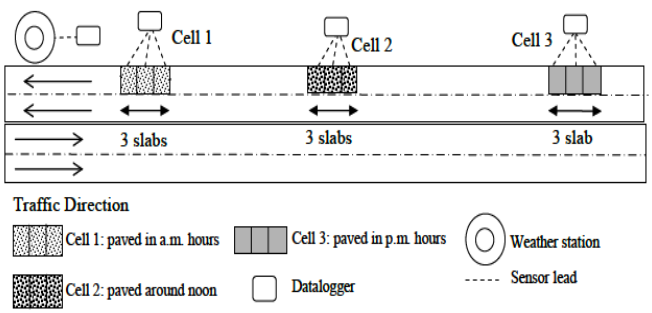

Fig. 2. Schematic Layout of the Three Cells Instrumented in Each Project.

To establish TZ for any JPCP with the same structure as the four instrumentation projects, the degree of hydration at TZ was established. It is known that for a particular mix, setting takes place at a certain degree of hydration [10]. This concept was previously used to identify final set for PCC mixtures [11] and is adopted in the current study to identify TZ. Degree of hydration can be defined as the ratio of the cumulative heat of hydration to the total heat released as a result [11]. The best-fit mathematical model to the test data for the degree of hydration has the form of the relation provided below:

Table 2. The As-built Depth of The Installed thermocouples for all Projects.

	Thermocouple Depths, cm					
	Cell 1		Cell 2		Cell 3	
	Slab A	Slab C	Slab A	Slab C	Slab A	Slab C
Project 1	2.0	2.3	1.5	2.0	3.3	2.0
	4.6	6.1	3.6	4.6	5.1	4.8
	9.7	9.1	6.1	8.1	8.6	8.6
	17.3	18.8	15.0	15.7	17.3	16.5
	27.4	28.4	26.9	27.2	28.7	27.9
	30.2	31.0	29.7	31.2	31.2	30.7
Project 2	1.0	0	2.3	4.8	1.0	2.0
	3.6	1.8	5.8	7.4	3.3	4.6
	7.4	4.3	9.1	11.2	6.6	8.6
	2.3	9.9	14.0	16.3	12.4	12.2
	11.2	17.3	21.3	23.4	19.3	20.6
	24.9	23.9	26.2	26.2	20.1	25.7
Project 3	0	1.0	4.8	2.8	2.0	2.3
	2.8	3.8	7.4	6.1	4.1	4.8
	5.8	7.9	10.9	9.9	7.9	8.6
	13.5	16.0	18.0	19.1	15.5	15.5
	25.1	26.7	29.7	29.2	27.7	26.2
	30.5	29.5	31.8	32.8	31.0	30.7
Project 4	9.9	14.2	5.1	3.8	5.8	6.1
	10.9	16.0	7.9	6.6	7.4	8.6
	15.2	19.3	11.4	17.3	12.2	12.4
	22.4	25.7	18.5	17.5	19.3	19.6
	33.0	37.8	30.5	29.5	30.0	31.2
	37.1	40.4	34.5	31.5	35.8	34.8

$$\alpha(t_\varepsilon) = \alpha_u \exp\left(\frac{\tau}{t_\varepsilon}\right)^{\beta} \quad (1)$$

where, α (t_ε) = degree of hydration; α_u = ultimate degree of hydration, t_ε = equivalent age and τ and β are time and hydration shape parameters. The respective relations for calculating τ, and β are available in the reference [12] and are not provided here. The two parameters are establishing based on the cement composition obtained from the mill sheet provided by the cement manufacturer. This information is summarized in Table 1, for the cement used on each project. The hydration progress was established for all slabs on all four projects during first few hours after construction. The degree of hydration at TZ was identified for all slabs and projects. The average value of 45 percent was found to represent the degree of hydration at TZ for all four instrumented projects. Since the pavement thickness varied between 9 to 15 inch (23- to 38 cm) among the four projects and the two typical PennDOT concrete paving mixtures used, it was concluded that JPCPs constructed in Pennsylvania with the same range of slab thickness will reach TZ at a degree of hydration of approximately 45 percent.

Establishing Built-in Temperature Gradients

A previous field study [9] showed that during hardening, the slab maintains a saturated condition throughout its cross section. Based on this observation, it is safe to assume that moisture gradients present in the slab at TZ are negligible. Therefore, the temperature distribution at TZ, measured along the depth of the slab suffices for establishing the built-in temperature gradient. When establishing this parameter though, it is essential to consider the nonlinearity in the temperature distribution along the slab depth. In doing so, the equivalent temperature gradient (ELTG) at TZ was estimated for each slab. In 2000, Janssen and Snyder [13] developed a relationship for estimating the *ELTG* based on the temperature moments in the slab as follows.

$$TM_0 = -0.25\left\{\sum_{i=1}^{n}(t_i + t_{i+1})(d_i^2 - d_{i=q}^2) - 2(d_1^2 - d_n^2)T_{WAT}\right\} \quad (2)$$

$$T_{WAT} = \sum_{i=1}^{n}\left[\frac{0.5(t_i + t_{i+1})(d_i - d_{i+1})}{(d_1 - d_n)}\right] \quad (3)$$

In the above equations, t_i = temperature at location i, °F; d_i = depth at location i, inch; T_{WAT} = weighted average temperature (WAT), °F. The temperature moment can be converted into an *ELTG* by determining the linear gradient that produces the same magnitude of temperature moment as the measured surface profile, using Eq. (4).

$$ELTG = \frac{-12(TM_0)}{h^3} \quad (4)$$

In this equation, h is slab thickness in inches. A summary of the built-in temperature gradients established for the three different cells in all four projects is presented in Fig. 3. In this figure, the cells are grouped based on time of paving. Four groups consisting of morning, noon, afternoon and late afternoon are defined. According to the Fig. 3, the lowest variability in the magnitude of the built-in temperature gradient is seen for the slabs paved during the morning and at noon. The largest variability is seen among the slabs paved in late afternoon. This could be because in the case of morning/noon paving, similar climatic conditions were present during the day for

Table 3. TZ Established for all Cells on all Projects Based on Strain-temperature Responses.

	Cell 1		Cell 2		Cell 3	
	Time of Paving	TZ (Hours after Placement)	Time of Paving	TZ (Hours after Placement)	Time of Paving	TZ (Hours after Placement)
Project 1	8:30	15.0	10:30	13.0	12:45	14.0
Project 2	8:00	22.0	12:00	20.0	15:45	20.0
Project 3	14:30	20.0	17:30	24.0	8:00	14.5
Project 4	8:30	24.5	14:30	16.0	16:45	17.0

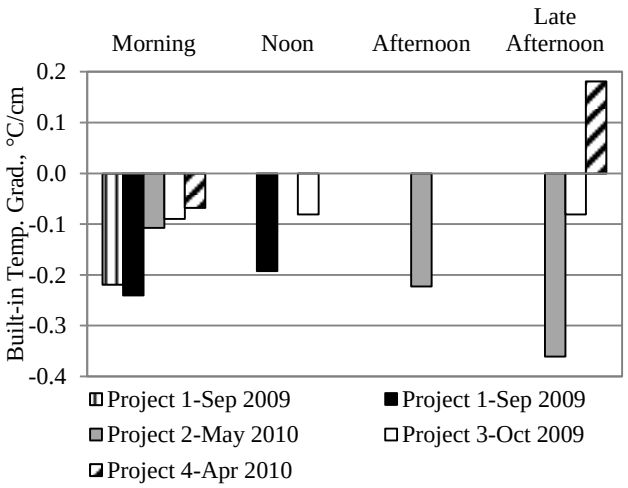

Fig. 3. Built-in Temperature Gradients Established for the Four Instrumented Projects.

the months the four projects were constructed. In the case of afternoon and evening paving, the climatic conditions varied depending on the time of paving. Cold conditions present in the afternoon decreased the rate of hydration of the cement. Depending on the rate of hydration, TZ can occur anytime during the night, resulting in a negative built-in gradient, or the next day, resulting in a positive temperature gradient.

This study aims at establishing the built-in temperature gradient without the need to instrument the slab with thermocouples. To achieve this goal, a numerical temperature model based on the general heat transfer equation is employed. The details regarding the temperature model are discussed as follows.

Numerical Temperature Model

Theory

The governing equation of heat transfer due to conduction presented in Eq. (5) in one dimensional domain, can be solved with respect to distance, *x*, and time, *t*, to predict temperature changes in the cross section of a pavement structure. In addition to the heat inflows and outflows, thermal energy is generated within the slab, which is the heat due to hydration of the cement.

$$\frac{d}{dx}\left(k\cdot\frac{dT}{dx}\right)+Q_H=\rho\cdot C_p\cdot\frac{dT}{dt} \quad (5)$$

In this equation, T = temperature, ℃; t = time, hours; ρ = density, kg/m3; C_p = specific heat, J/kg/℃; Q_H = generated heat per unit time and volume, W/m^3; k = thermal conductivity, W/m/℃. The temperature in the PCC is determined by the balance between the heat generation in the PCC and the heat exchange with the environment. Heat transfer to the surroundings occurs in five different ways: conduction, convection (q_c), irradiation (q_r), solar absorption (q_s) and evaporation. It must be noted that the cooling of the surface due to evaporation was not considered in this study. The boundary conditions defined at the top of the pavement section is presented in Eq. (11) [14]. At the bottom, a constant temperature of 12℃ was assumed at a depth of 100 inches [15]. Models already available in literature for defining each of the four heat transfer mechanisms at the boundary conditions were used in this study. A summary of these models is provided in Table 4. The required input parameters for the models, such as solar radiation, wind speed and ambient temperature were measured at the site.

$$-k\nabla T.n+q_c+q_r-q_s=0 \quad (11)$$

The hydration reaction of Portland cement is an exothermic process. Therefore, when using the general heat transfer equation, presented in Eq. (5), to predict the temperature variations across the pavement structure, the rate of heat liberation, Q_H, needs to be considered for each time step. The regression model developed in 2005 by Schindler and Folliard [12] was used for this purpose.

$$Q_H=H_u C_c\left(\frac{\tau}{te}\right)^{\beta}\left(\frac{\beta}{te}\right)\alpha(te)\exp\left[\frac{-E}{R}\left(\frac{1}{273+T_c}-\frac{1}{273+Tr}\right)\right] \quad (12)$$

$$H_u=H_{cem}P_{cem}+461P_{slag}+1800P_{Cao\text{-}FA}\cdot P_{FA} \quad (13)$$

$$H_{cem}=500PC3A+260PC2S+866PC3S+420PC4AF+624PSO3+1186Pfree\text{-}Cao+85PMgO \quad (14)$$

where, Q_H = rate of heat liberation, W/m^3; Hu = total heat of hydration of cementitious materials at 100 percent hydration, J/kg, Cc = cementitious materials content, kg/m^3, E = Activation energy,

Table 4. Models Used to Define The Boundary Conditions for The Heat Transfer Model.

Heat Transfer Mechanism	Corresponding Model		Definition of Parameters	Reference
Convection	$q_c=h_c(T_c-T_a)$	(6)	q_c = Convection Heat Flux W/m^2, h_c = Surface Convection Coefficient, kJ/m^2/h/℃ Tc = Concrete Surface Temperature, ℃ T_a = Surrounding Air Temperature, ℃.	[16]
	If $w \le 5$ m/s: $h_c = 20 + 14w$ else: $h_c = 25.6*0.78w$	(7) (8)	w = Wind Velocity, m/s	[17]
Solar Absorption	$q_s=\beta.q_{solar}$	(9)	q_s = Solar Absorption Heat Flux W/m^2, β = Solar Absorptivity = 0.5 for Concrete, q_{solar} = Instantaneous Solar Radiation, W/m^2	[18-19]
Irradiation	$q_r=\varepsilon[4.8+0.075.(T_a-5).(T_c-T_a)]$	(10)	q_r = Heat Flux of Heat Emission from The Surface, W/m^2 ε = Surface Emissivity of Concrete = 0.88	[19]

J/mol, R = Universal gas constant, 8.3144 J/(mol K). In Eq. (13), H_{cem} = total heat of hydration of cement derived from Eq. (14), P_{cem} = cement weight ratio in terms of the total cementitious content, P_{slag} = slag weight ratio in terms of the total cementitious content, $P_{Cao\text{-}FA}$= mass ratio of Cao in fly ash to total fly ash content, PFA = weight ratio of fly ash out of total cementitious content. In Eq. (14), PC3A = weight ratio of tricalcium silicate in terms of the total cementitious content, PC2S = weight ratio of dicalcium silicate in terms of the total cementitious content, PC4AF = weight ratio of tetracalcium aluminoferrite in terms of the total cementitious content, PSO3 = weight ratio of sulfur trioxide in terms of the total cementitious content, PCao = weight ratio of free lime in terms of the total cementitious content, PMgO = weight ratio of magnesia in terms of the total cementitious content.

Q_H, as seen in Eq. (5), depends on the temperature of the slab. Using the finite difference method to develop step-by-step solutions for Eq. (5) made it possible to incorporate the hydration model into the temperature prediction analysis. The conductivity of concrete was defined as a fraction of the degree of hydration. An empirical relation is available that provides a linear relation between the k of concrete and the degree of hydration [16]. This relation is provided in Eq. 15.

$$k = k_{\infty}\left(1.33 - 0.33\alpha\right) \tag{15}$$

where, k = current thermal conductivity of concrete, W/m/℃, k_{∞} = thermal conductivity of mature concrete selected based on typical values suggested in the reference, W/m/℃. The relation provided in Eq. (16) was used for establishing C_p of the mixture. This relation includes the effects of proportioning and specific heat of each constituent together with the degree of hydration in establishing the C_p for concrete [17-18]:

$$Cp = \frac{1}{\rho}\left(W_c \alpha C_{cef} + W_c\left(1-\alpha\right)Cc + Wa.Ca + W_w.C_w\right) \tag{16}$$

where, C_p = current specific heat of concrete, J/kg/℃, W_c = amount by weight of cement , kg/m^3, W_a = amount by weight of aggregate, kg/m^3, W_w = amount by weight of water, kg/m^3, C_{cef} = fictious specific heat of the hydrated cement determined as 8.4 T_c+339 where T_c is the current concrete temperature in ℃, C_c = specific heat of cement, J/kg/℃, C_a = specific heat of aggregate, J/kg/℃, C_w = specific heat of water, J/kg/℃, selected based on typical values suggested for these material in the references [17-18].

Table 5. Values Used for Inputs into the Temperature Model for Project 1.

Category	Parameter	Value
Time and Space Steps	Δx (cm)	3
	Δt (Seconds)	Varies
	Initial Temperature of Concrete, ℃	17
Nodes	Nodes in PCC Slab (No.)	10
	Nodes in Base Layer (No.)	3
	Nodes in Sub-base Layer (No.)	5
	Nodes in Subgrade Layer (No.)	45
Thermal Conductivity	k_{∞} of Concrete (W/m/℃)	2
	k of Base Layer (W/m/℃)	1.38
	k of Sub-base Layer (W/m/℃)	2.42
Weather Data	Temperature, Wind Speed, Precipitation, Solar Radiation	Measured at the Site
Analysis Time	Time (Hours)	72

Comparison of Predictions with Field Data

Temperature throughout the depth of the instrumented slabs in all projects was predicted for the first 72 hours after construction. The results for the three cells in each project will be presented in the form of the ELTG estimated using the Janssen-Snyder method discussed previously. The ELTG estimated based on measured temperature data throughout the slabs in each cell is used to evaluate the validity of the predictions from the model. The as-built depth of the thermocouples in each slab is summarized for each project in Table 2. These depths were established through pre- and post-slab construction surveys. The general inputs used to define the required inputs for the model are provided in Table 5.

Project 1

Project 1 consisted of Cells 1, 2 and 3, paved at 8:00, 10:30 and 12:30 AM, respectively on 9/2/2009. Unfortunately, the time of paving was exceptionally close for all cells on this project. Even though the location of each cell was established based on discussions with the contractor, the unpredictability of the paving production rate on the day of paving resulted in paving all three cells at similar times of the day.

The ELTG estimated based on both thermocouple data and model predicted values are presented in Fig. 4 a, b and c for the three cells on this project together with the ambient temperature measured at the site. As seen in the figures, the ELTG predicted using the model agrees very well with the ELTG established based on field data. Slight differences between the two could be due to differences in the depth of the thermocouples and the fineness of the mesh used for modeling the slab. Also, it is noticeable in Fig. 4 b and c that for Cells 2 and 3, the model predictions deviate slightly from the field data during the first six hours after paving. When predicting temperature behavior of a mixture during early ages, the best results are obtained when the hydration shape and time parameters for the mixture are established through semi-adiabatic calorimeter testing. Unfortunately, this equipment was not available for this study. Additionally, the possible effect of the water content is not considered in the hydration model presented in Eq. (12). Based on Table 1, Cells 2 and 3, which show more variability in the predicted temperatures, were paved with PCC mixtures with a high w/cm ratios of 0.48 and 0.47, respectively. Cell 1, on the other hand, was made of PCC with a w/cm ratio of 0.41. It is expected that higher water content can delude more of the heat released during hydration.

Project 2

Project 2 also included three instrumented cells, paved at 8:30, 12:00 and 15:45 on 5/10/2010. The ELTG estimated based on the

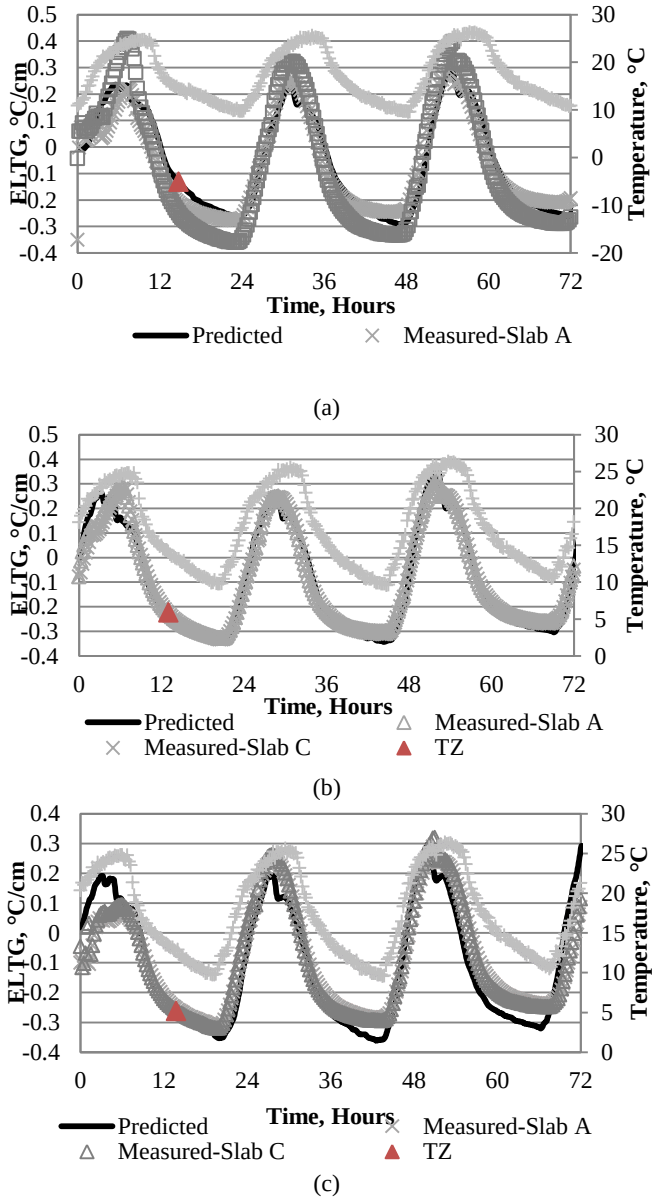

Fig. 4. ELTG Estimated Based on Field Measurements and Model Predicted Temperatures for Project 1 (a) Cell 1 Paved at 8:00, (b) Cell 2, Paved at 10:30 and (c) Cell 3 Paved at 12:45.

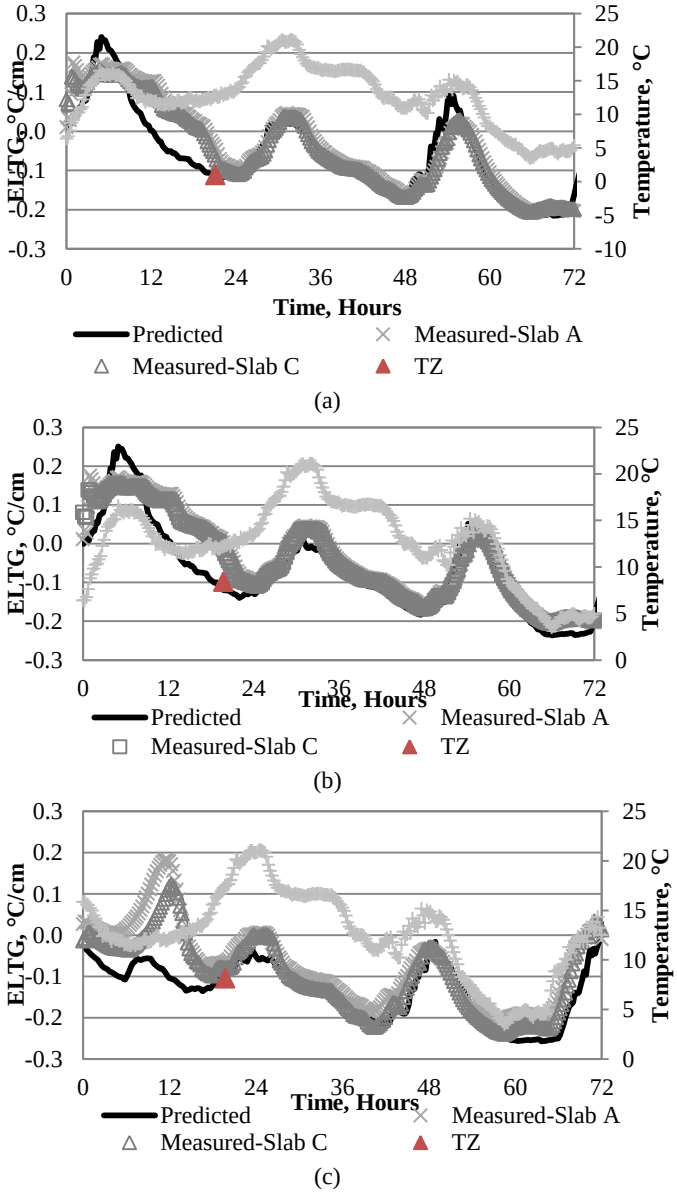

Fig. 5. ELTG Estimated Based on Field Measurements and Model Predicted Temperatures for Project 2 (a) Cell 1 Paved at 8:30 AM, (b) Cell 2 Paved at 12:00 and (c) Cell 3 Paved at 15:45.

predicted temperatures across the slab together with the ELTG estimated based on the measured data is presented in Fig. 5 a, b and c for the three cells on this project. It is noteworthy that the paving day for this project was relatively cold and completely overcast. The rain started at about 16:30, which resulted in the complete coverage of the slabs with plastic sheets. The exact time when the plastic sheets were removed from the slabs is not known. Based on Fig. 5 though, it appears that the plastic covers influence the predicted ELTG up until about 24 hours after the placement of the slabs in Cells 1 and 2 and 12 hours in Cell 3. The predictions for the ELTG at TZ, however do not appear to be significantly influenced by this phenomenon, especially in Cells 1 and 3. Based on the figures, it is also noticed that the behavior of the slab in terms of ELTG is completely the same for Cells 1 and 2.

Project 3

The time of paving for the cells on Project 3 were different from other projects in the sense that Cell 1 was paved at 14:30, Cell 3 at 17:30 on 4/29/2010 and Cell 3 at 8:30 on 4/30/2010. The ELTG based on the predicted values together with the ELTG based on the field data are presented in Fig. 6 a, b and c. Based on these figures the predicted values agree relatively well with the field data in all cells.

Project 4

This project was constructed on 5/7/2010, with Cell 1 paved at 7:30, Cell 2 paved at 14:30 and Cell 3 at 16:30. The ELTG estimated based on the predicted temperatures and also the ELTG calculated

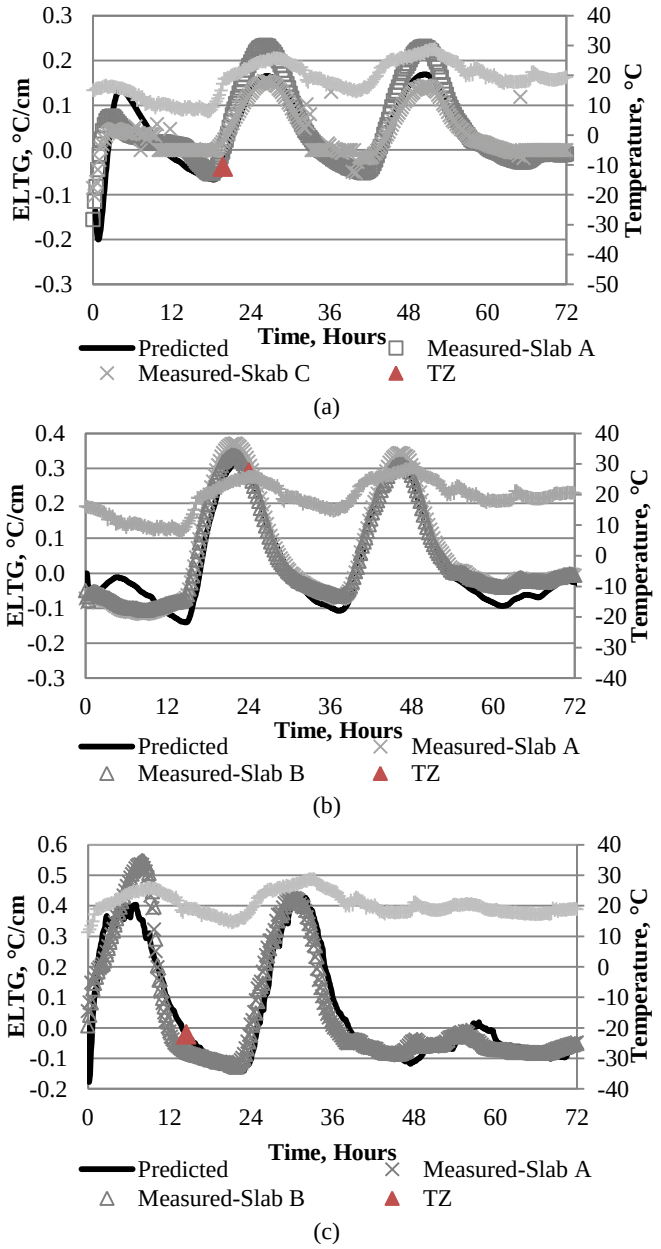

Fig. 6. ELTG Estimated Based on Field Measurements and Model Predicted Temperatures in Project 3 (a) Cell 1, Paved at 14:30, (b) Cell 2 Paved at 17:30 and (C) Cell 3, Paved at 8:30.

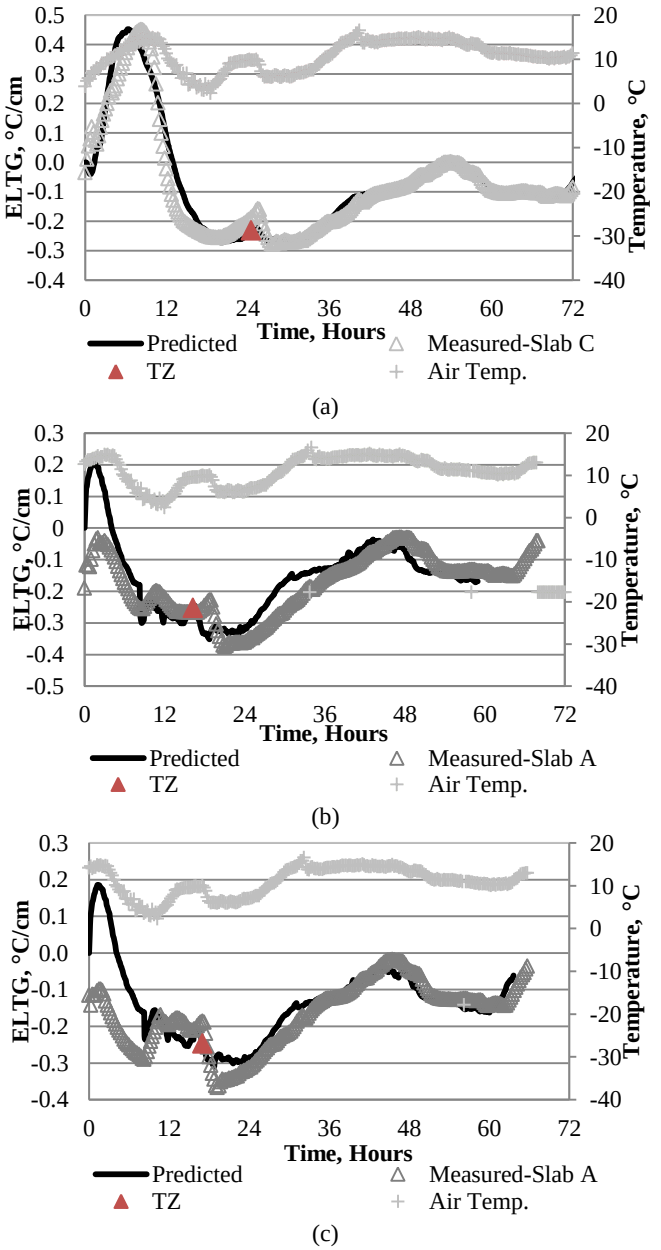

Fig. 7. ELTG Estimated Based on Field Measurements and Model Predicted Temperatures in Project 4 (a) Cell 1, Paved at 8:00 AM, (b) Cell 2 Paved at 14:30 and (C) Cell 3, Paved at 16:30.

based on the measured data is presented in Fig. 7 for all three cells for this project. The predicted values agree very well with the thermocouple data in Cell 2, while it is over-predicted for the first 10 hours for the PM cells. It is also interesting to note that the ELTG behavior of Cells 2 and 3 paved in the afternoon are similar to each other but different from Cell 1, which was paved in the morning.

Characterizing Climatic Conditions

Establishing Climatic Regions

To use the temperature model to predict the temperature behavior of a pavement section, a reliable climatic database compiled based on at least 10 years of data is required. The MEPDG includes a total of 23 climatic databases from weather stations in different counties across Pennsylvania. In an effort to establish the built-in temperature gradient for the pavement sections constructed at different locations in the state, the entire state was divided into climatic regions.

The climatic regions were defined mainly based on the variation in elevation, freezing index (FI) and annual air temperature. The climatic databases available for Pennsylvania in the MEPDG software were used to establish the major climatic indices, such as annual air temperature, rainfall, wind speed, RH and FI for each database. The FI for each climatic station together with their elevations are presented in Fig. 8. The mean annual air temperature for each climatic station together with the elevations of the stations is presented in Fig. 9. As shown in these two figures with red circles,

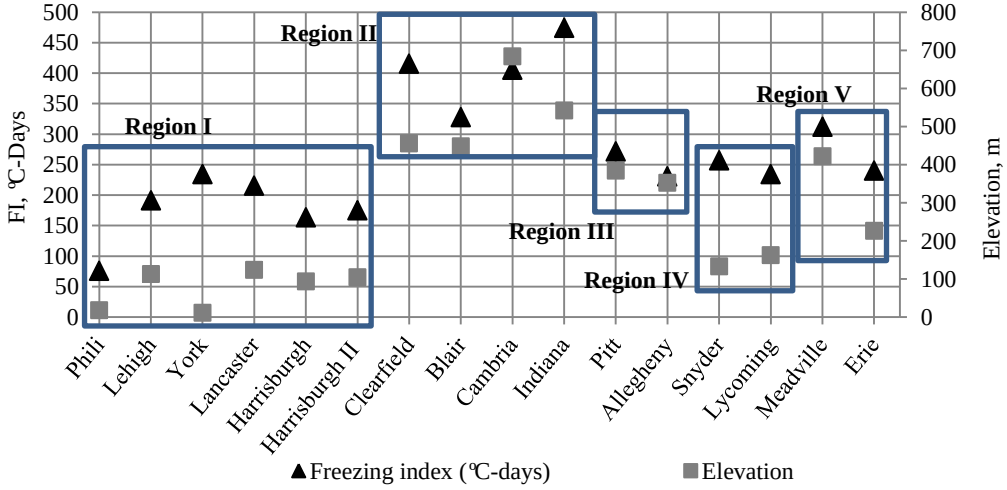

Fig. 8. Five Climatic Regions Based on The FI and Elevation of the Climatic Stations Available in The MEPDG.

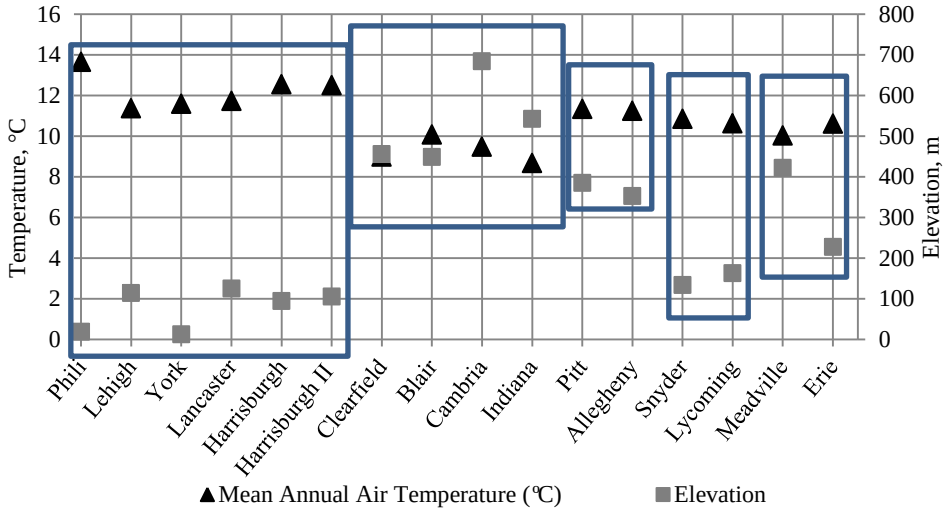

Fig. 9. Climatic Regions Based on The Mean Annual Air Temperature and Elevation of the Climatic Stations Available in The MEPDG.

the stations with similar elevations, FI and mean annual air temperature were grouped together. Five different climatic regions were established for the state. The different climatic regions are shown with the red circles in Fig. 8 and Fig. 9. The five different regions were also presented on a county map for the state in Fig. 10. The range for the FI, mean annual air temperature and elevation in each climatic region is summarized in Table 6. The five climatic regions established in this section do not include all the counties in the state as seen in Fig. 10. The proper climatic region needs to be assigned to each county based on the ranges provided in Table 6 for FI, mean annual temperature and elevation and based for each region. The FI is available for each county in Pennsylvania in the PennDOT Pavement Policy Manual, Publication 242, Appendix D. The mean annual temperature for each county can also be extracted from the National Oceanic and Atmospheric Administration (NOAA) website.

A climatic database was compiled for each of the five climatic regions discussed above. This was accomplished by taking the average of the hourly climatic data for the stations in each region over one year. The one year data was then averaged over the years that the data was available (minimum of five years). The established climatic database for each region can then be incorporated into the validated numerical temperature model discussed earlier to find the temperature gradient at TZ in the slabs constructed in different locations in Pennsylvania.

Month, Day and Time of Paving

Since the designer can only guess the month of construction of the section, this parameter is very unlikely to be defined accurately at the time of design of the section. Therefore, the sensitivity of the month of construction to the predicted built-in temperature gradient needs to be investigated.

The built-in temperature gradient was established for the slabs constructed on the first day of every month over the construction season, using the climatic database for Region 1 and the average critical degree of hydration of 0.45. The results are presented in Fig. 11 in the form of seasonal averages. The error bars in this figure show the variability in the built-in temperature gradient within each season.

Since the construction season does not start until the warmer days in March, the colder days of this month were not included in the

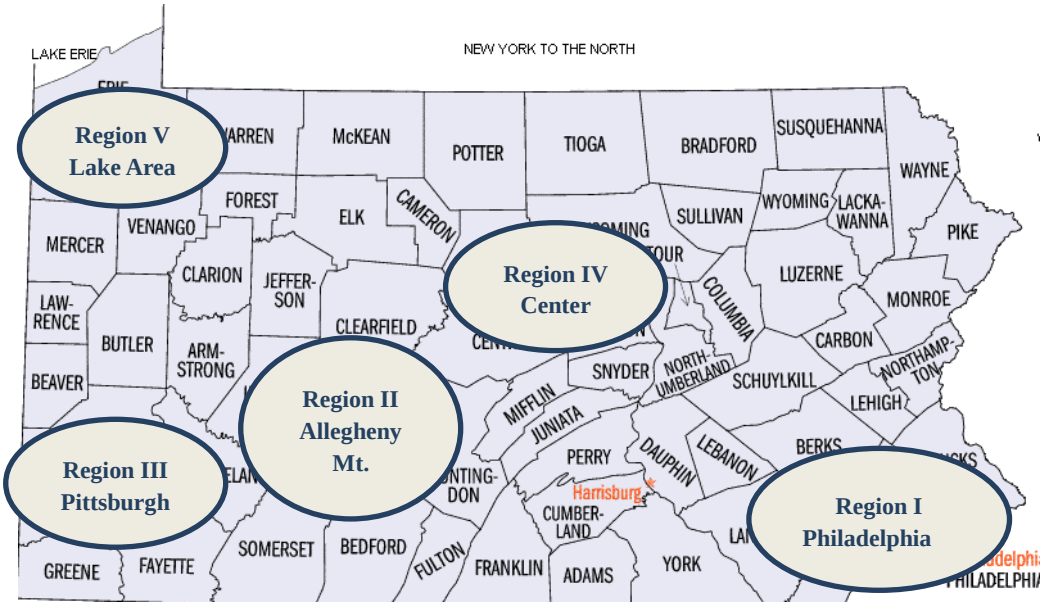

Fig. 10. Climatic Regions on the County Map for Pennsylvania, (source: http://www.censusfinder.com/mappa.htm).

Table 6. Ranges for FI, Mean Annual Air Temperature and Elevation for Each Climatic Region.

Region/Range	Region I		Region II		Region III		Region IV		Region V	
	Min	Max	Min	Max	Min	Max	Min	Max	Min	Max
Mean Annual Air Temp., ℃	11	14	9	10	11	11	11	11	10	11
Freezing Index, ℃-days	76	234	328	475	231	272	234	257	240	312
Elev., m	12	125	449	684	353	384	133	163	227	422

Table 7. Built-in Temperature Gradient (℃/cm) for the Five Climatic Regions in the State.

Month of Construction	Slab Thickness				
	20 cm	27 cm	30 cm	33 cm	36 cm
April	-0.6	-0.6	-0.6	-0.6	-0.6
May	0.1	0.0	-0.1	-0.1	-0.1
July	0.3	0.2	0.2	0.1	0.1
Sep.	0.0	0.0	0.0	-0.1	-0.1
Oct.	0.1	0.0	0.0	-0.1	-0.1
Nov.	-0.7	-0.6	-0.6	-0.6	-0.6

study. It is also noteworthy that spring was defined to include months of March, April and June. Based on Fig. 11, the largest positive temperature gradient is seen during the summer. This agrees with expectations, since the high ambient temperatures and solar radiant in the summer results in an increase in the rate of hydration of the cement in comparison to paving in colder days of fall or spring. Therefore, a slab paved at 8:00 AM, reaches TZ sometime during the hot summer afternoon and will then lock in a large positive built-in temperature gradient. In the fall or spring, on the other hand, a slab paved in the morning would reach TZ during the cooler time of the day and therefore, the built-in temperature gradient can be negative and the magnitude is relatively small.

Furthermore, a high variability is seen in the built-in temperature gradient for the months in the spring and the fall, as expected, while a very low variability is seen over the summer. Therefore, the built-in temperature gradient needs to be established for only one month during the seasons with a low variability. This parameter will be established for all three months in the seasons with a high variability (spring and fall).

The effects of slab thickness on the built-in temperature gradient were also investigated. The temperature model was used to establish the built-in temperature gradient for PCC slabs ranging between 8 inches (20 cm) and 14 inches (36 cm), constructed in Region II in different months during the construction season. The results are summarized in Table 8. Based on the table, slab thickness does not affect the built-in temperature gradient significantly regardless of the month of construction. This means that the values established in this study for the built-in temperature gradient can be used for pavements with slab thicknesses ranging between 9 inch (23 cm) and 14 inch (35.5 cm) (this is the range seen among the four instrumented projects).

Based on the data from the four instrumented projects, the trend in the ELTG is similar for the sections paved during the period between the morning and noon. The ELTG is not consistent with

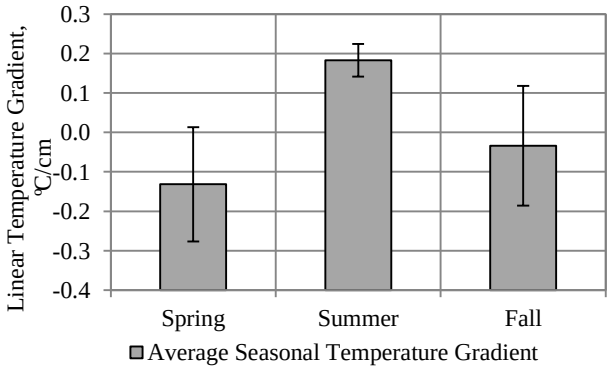

Fig. 11. Average Seasonal Built-in Temperature Gradient for Different Seasons.

Table 8. Built-in Temperature Gradient (℃/cm) for The Five Climatic Regions in The State.

Month of Construction/ Climatic Region	March	April	May	July	Sep.	Oct.	Nov.
Region I	-0.2	-0.1	0.1	0.1	0.1	0.1	0.0
Region II	-0.3	-0.1	0.0	0.1	0.1	0.0	-0.1
Region III	-0.3	-0.1	0.0	0.1	0.1	0.0	-0.1
Region IV	-0.2	-0.1	0.1	0.1	0.1	0.1	0.0
Region V	-0.3	-0.2	0.0	0.1	0.1	0.1	-0.1

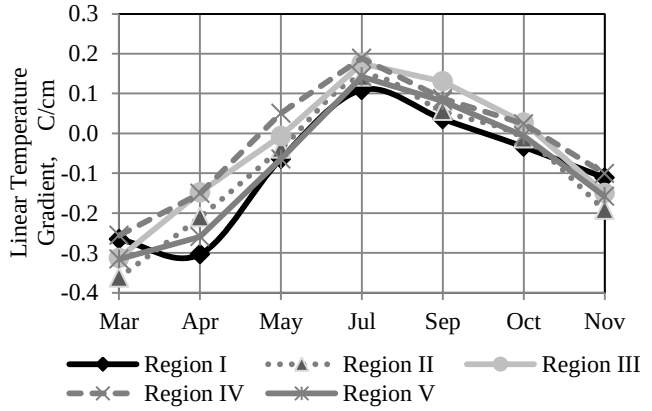

Fig. 12. Built-in Temperature Gradient for Five Different Regions in PA, for Gradient Construction Month and Time of Paving of 8:00 AM.

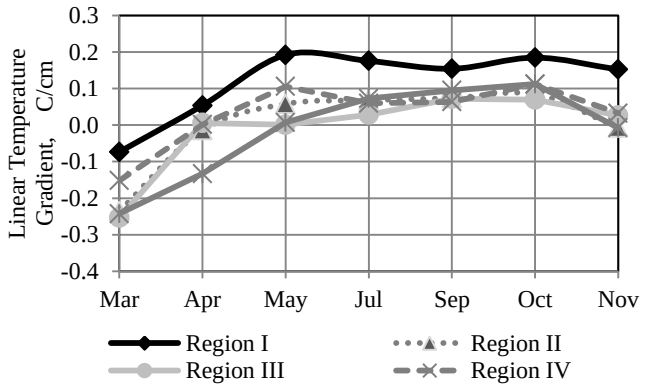

Fig. 13. Built-in Temperature Gradient for Five Different Regions in PA, for Gradient Construction Month and Time of Paving of 5:00 PM.

that obtained when paving takes place in late afternoon. Based on this observation, the built-in temperature gradient is established for pavement sections constructed in Pennsylvania in different months during the construction season and at two times during the day, once at 8:00 AM and the other at 5:00 PM. The built-in temperature gradient for the slabs paved in the morning and paved in the afternoon are presented in Fig. 12 and Fig. 13, respectively. The average of the built-in temperature gradient in the two figures is summarized in Table 8.

Based on the data from Table 8, the built-in temperature gradients for Region I are similar to the ones established for Region IV in all months. These two regions are two neighboring regions on the county map in Fig. 10 and can be combined into one climatic region, named Climatic Region A. Also, based on the data from Table 8, Regions II and III show similar values for the built-in temperature gradient in almost all months. These two regions are again neighboring regions on the county map presented in Fig. 10 and can be combined into one climatic region, named Climatic Region B. Region V, or the lake region, is referred to as Climatic Region C. The final average built-in temperature gradients are summarized in Table 9 for Climatic Regions A, B and C. As seen in Table 9, the highest value of -0.3℃ is seen for the built-in temperature gradient for the sections constructed in Regions II and III in the Month of March. During April, the built-in temperature gradients remain relatively high in the two regions. While in other months in the construction season, the built-in temperature gradient reaches the magnitudes of either 0.1 or zero.

The default value of -5.5℃ (-10 ℉) is used in the MEPDG for the permanent effective curl/warp temperature gradient. This value was established through optimization of the cracking model for the Long-Term Pavement Performance (LTPP) sections across the nation. While the generalization of ambient conditions for different counties across the state and using representative climatic databases can be a source of error in the proposed method, the results still better reflect local conditions when compared with the MEPDG default value. This proposed method incorporates the effects of local conditions (PCC design mixture, time and month of paving and ambient conditions) when establishing the built-in temperature gradient. It should be remembered though, that the value of -5.5℃ (-10℉) used in the MEPDG represents the effects of both permanent curling and warping and cannot be compared to the values established herein.

Conclusions

This study presented an effort toward estimating proper values for the built-in temperature gradient for JPCPs constructed in Pennsylvania. First, TZ was established for four instrumented paving projects in Pennsylvania. This was performed based on the strain-temperature behavior of the hardening concrete slabs on each project. The degree of hydration was estimated at TZ for all projects. The average degree of hydration among all projects was recommended to be used to identify TZ in concrete pavements constructed in Pennsylvania. A numerical temperature model was employed and validated, based on field temperature data from four paving projects. The ELTG established based on the model's temperature predictions at different depths of the slabs agreed very well, especially at TZ, for cells paved during AM hours. When paving was performed in the PM hours, some variation was observed between the predicted ELTG and the measured ELTG during first few hours after paving. There was agreement between the two projects at around TZ. To be able to recommend typical values for the built-in temperature gradient for pavement sections constructed in Pennsylvania, the state was divided into five climatic

Table 9. Built-in Temperature Gradient (℃/cm) for the Three Final Climatic Regions in the State.

Month of Construction/ Climatic Region	March	April	May	July	Sep.	Oct.	Nov.
Region A	-0.2	-0.1	0.1	0.1	0.1	0.1	0.0
Region B	-0.3	-0.1	0.0	0.1	0.1	0.0	-0.1
Region C	-0.3	-0.2	0.0	0.1	0.1	0.1	-0.1

regions. These five regions were later merged to define only three major climatic regions within the state based in similarities observed between several regions. A representative climatic database was generated for each climatic region, and then used along with the numerical model to establish the ELTG at TZ. The built-in temperature gradient was established for JPCPs constructed in each of the climatic regions for each month within the construction season at two different times of the day. The method is simple and can be easily incorporated into the MEPDG. It considers the effects of climatic conditions during paving and the PCC mixture design.

Acknowledgements

This study was performed as part of Project Work Order#13, Contract # 510601, funded by the Pennsylvania Department of Transportation (PennDOT) The authors would like to express their appreciation for both the financial and technical support provided by PennDOT. Also the efforts of all graduate students at the University of Pittsburgh who assisted with the field work and laboratory testing associated with this project is greatly appreciated.

References

1. Armaghani, J.M., Larsen, T.J., and Smith, L. (1987). Temperature Response of Concrete Pavements, *Transportation Research Record*, No. 1121, pp. 22-33.
2. Eisenmann, J. and Leykauf, G. (1990). Simplified Calculation Method of Slab Curling Caused by Surface Shrinkage, *Proceedings of 2nd International Workshop on Theoretical Design*, Siquenza, Spain.
3. Janssen, D.J. (1987). Moisture in Portland Cement Concrete, *Transportation Research Record*, No. 1121, pp. 40-44.
4. Burnham, T. and Koubaa, A. (2001). A New Approach to Estimate the In-situ Thermal Coefficient and Drying Shrinkage for Jointed Concrete Pavements, *7th International Conference on Concrete Pavements*, Orlando, Florida, USA.
5. Yu, H.T. and Khazanovich, L. (2001). Effects of Construction Curling on Concrete Pavement Behaviour, *7th International Conference on Concrete Pavements*, Orlando, Florida, USA.
6. Nassiri, S. and Vandenbossche, J.M. (2010). Establishing Appropriate Inputs When Using the MEPDG to Design Rigid Pavements in Pennsylvania-Task 5-Establishing the Built-in Gradient, *Prepared for Pennsylvania Department of Transportation*, University of Pittsburgh, Pittsburgh, Pennsylvania, USA.
7. ARA Inc. ERES Consultants Division (2004). Guide for Mechanistic-Empirical Design of New and Rehabilitated Pavement Structures, *National Cooperative Highway Research Program*, Transportation Research Board, Champaign, Illinois, USA.
8. Rao, C., Titus-Glover, L., Bhattacharya, B.B., and Darter, M. (2011). Estimation of DeltaT Input for JPCP Design Using the MEPDG, *Proceedings of the 90th Annual Meeting of Transportation Research Board*, Washington, DC., USA.
9. Wells, S.A., Phillips, B.M., and Vandenbossche, J.M. (2006). Quantifying Built-In Construction Gradients and Early-Age Slab Deformation Caused by Environmental Loads in a Jointed Plain Concrete Pavement, *International Journal of Pavement Engineering*, 7(4), pp. 275-289.
10. Byfors, J. (1980). Plain Concrete at Early Ages, Swedish Cement and Concrete Research Institute.
11. Schindler, A.K. (2004). Prediction of Concrete Setting, *Proceedings of the RILEM Conference on Advances in Concrete through Science and Engineering*, Evanston, Illinois, USA.
12. Schindler, A.K. and Folliard, K.J. (2005). Heat of Hydration Models for Cementitious Materials, *ACI Materials Journal*, 102(1), pp. 24-33.
13. Janssen, D.J. and Snyder, M.B. (2000). The Temperature-Moment Concept for Evaluating Pavement Temperature Data, *Journal of Infrastructure Engineering*, 6(2), pp. 81-83.
14. Jeong, J.H., Wang, L., and Zollinger, D.G. (2001). A Temperature and Moisture for Hydration Portland Cement Concrete Pavements, *International Conference on Concrete Pavements*, Orlando, Florida, USA.
15. Hermansson, A. (2001). Mathematical Model for Calculation of Pavement Tempatures, *Transportation Research Record*, No. 1764, pp. 180-188.
16. Solaimanian, M. and Kennedy, T.W. (1998). Predicting Maximum Pavement Surface Temperature Using Maximum Air Temperature and Hourly Solar Radiation, *Transportation Research Record*, No. 1417, pp. 1-11.
17. Ruiz, J.M., Rasmussen, R.O., Chang, G.K., Dick, J.C., Nelson, P.K., Schindler, A.K., Turner, D. J., and Wilde, W. J. (2006). Computer-Based Guidelines for Concrete Pavements, Volume III: Technical Appendices, *FHWA-HRT-04-127*, Wasginton, DC., USA.
18. Jeong, J.H. and Zollinger, D.G. (2005). Environmental Effects on the Behavior of Jointed Plain Concrete Pavements, *Journal of Transportation Engineerg*, 131(2), pp. 140-148.
19. Ruiz, J.M., Schindler, A.K., Rasmussen, R.O., Nelson, P.K., and Chang, G.K. (2001). Concrete Temperature Modeling and Strength Prediction Using Maturity Concepts in the FHWA HIPERPAV Software, *7th International Conference on Concrete Pavements*, Orlando, Florida, USA.